Physicochem. Probl. Miner. Process., 61(4), 2025, 204867

http://www.journalssystem.com/ppmp

Physicochemical Problems of Mineral Processing

ISSN 1643-1049

Flotation separation of fine scheelite and calcite by microbubbles using gum arabic as depressant

Xianping Luo [1,2,3], Hao Xu [1,2], Wei Guo [1,2], Jinrui Zhou [1,2], ZongKang Li [1,2]

[1] Jiangxi Province Key Laboratory of Mining and Metallurgy Environmental Pollution Control, Jiangxi University of Science and Technology, Ganzhou 341000, China

[2] Faculty of Resource and Environmental Engineering, Jiangxi University of Science and Technology, Ganzhou 341000, China

[3] School of Water Resource and Environmental Engineering, East China University of Technology, Nanchang, 330013, China

Corresponding author: guowei2667@qq.com (Wei Guo)

Abstract: This study examined the role of gum arabic (GA) as a depressant in the flotation separation of fine-grained scheelite and calcite using flotation and adsorption tests, Zeta potential and contact angle measurements, and X-ray photoelectron spectroscopy (XPS). Microbubbles were introduced to improve the flotation separation of scheelite and calcite, addressing the poor flotation performance of fine-grained minerals. In the pH 9 slurry, GA significantly depress calcite while having minimal effect on scheelite. A concentrate with a WO_3 grade of 60.47% and a recovery of 74.29% was achieved using GA and sodium oleate as the depressant and collector for a 1:1 mixed mineral. Adsorption tests indicated that scheelite adsorbed less GA on its surface compared to calcite. Contact angle measurements demonstrated that GA altered calcite's wettability, rendering it hydrophilic. XPS analysis indicated that GA formed a chemical interaction with the surface Ca^{2+} ions of calcite, whereas it exhibited weak physical adsorption on scheelite. Zeta potential measurements revealed selective chemical adsorption of GA anions on fine-grained calcite surfaces. In conclusion, the inhibition mechanism of GA on calcite is related to the chemical chelation with surface Ca^{2+}, enabling the efficient flotation separation of fine-grained scheelite and calcite, and the introduction of microbubbles can enhance the recovery of scheelite.

Keywords: fine particles, scheelite, calcite, gum arabic, microbubbles

1. Introduction

Froth flotation is a prevalent technique for scheelite beneficiation (Kupka and Rudolph., 2018; Lu et al., 2023; Ben Said et al., 2024). Currently, coarse-grained minerals that are easy to sort are scarce, facing the challenge of recovering fine-grained minerals. The traditional flotation method has limitations in effectively recovering fine particle minerals. First, in the conventional flotation process, the collision efficiency between fine particles and bubbles is relatively low, and the rising speed is slow. Additionally, fine particles tend to agglomerate during separation, leading to decreased separation efficiency. Second, existing separation equipment is often designed for specific particle sizes and mineral characteristics, making it challenging to address the separation needs of fine scheelite and calcite simultaneously. Furthermore, the selection and dosage of flotation reagents must be precisely controlled to minimize environmental effect (Miettinen et al., 2010; Dong et al., 2025). Recent studies indicate that incorporating microbubbles in flotation enhances the flotation performance of fine-grained minerals. In the field of flotation, three types of bubbles are defined based on the size of microbubbles: (1) microbubbles: with a diameter of less than several hundred micrometers, (2) micro-nano bubbles: with a diameter between 0.1 to 50μm, and (3) nano bubbles: with a diameter between 10 to 100nm (Chang et al., 2023). The effect of microbubbles on flotation performance is multifaceted. First, microbubbles selectively nucleate/adsorb on the surface of hydrophobic minerals, increasing the selective differences between

DOI: 10.37190/ppmp/204867

minerals and aiding in the improvement of concentrate grade. Second, the introduction of microbubbles reduces the average size of bubbles in the flotation system, increasing the probability of collisions between bubbles and particles; the nucleation/attachment of microbubbles on mineral surfaces facilitates the interaction between bubbles and particles, enhancing the probability of bubble/particle attachment, thereby improving the recovery rate of mineral flotation (Li et al., 2015). Rulyov et al. find the effectiveness of microbubbles in applications is influenced by their size and the concentration of the collector/frother used to generate them. Wei et al. research on microbubble flotation for fine black tungsten ore demonstrated an 85% recovery rate, approximately 15% higher than conventional flotation methods. This finding suggests that the likelihood of collision and adhesion between fine particles and smaller bubbles is higher, enhancing the floatability of fine minerals. In the flotation of fine-grained scheelite, Ji et al. used a cyclone-static microbubble flotation column to obtain a recovery of 79.02% for scheelite concentrate, which is about 1.6 times higher than that of conventional processes. Huang et al. developed a new type of microbubble flotation column, with bubbles in the flotation column having a diameter of 400μm, significantly increasing the flotation rate constant for fine-grained scheelite, allowing for effective recovery of fine-grained scheelite. Efficiently separating scheelite from other calcium-bearing gangue minerals is challenging due to their highly similar physical and chemical properties (Peng et al., 2024; Qiao et al., 2024). Calcite, a prevalent calcium carbonate gangue mineral, is considered to adversely affect scheelite enrichment during the hydrometallurgical process (Faramarzpour et al., 2022). Therefore, the separation of calcite from scheelite is of great significance for cost-saving in the hydrometallurgical process.

Fatty acids and their derivatives are the predominant collectors in scheelite flotation due to their strong adsorption on scheelite surfaces via interaction with exposed calcium ions (Wang et al., 2016; Filippov et al., 2018; Fawzy,2018). Due to the presence of calcium ions in the cleavage of calcite and scheelite, the selective collection ability of fatty acids in scheelite flotation is poor. Wang et al. believed fine-grained calcite has a larger surface area and higher surface energy, exhibiting stronger reactivity with reagents than scheelite, which complicates the flotation separation of the two. Achieving the separation of scheelite from calcite in flotation processes using only fatty acids, without suitable depressants, is challenging in practical applications. Industrial depressants are typically inorganic, such as sodium silicate and its solutions with metal ions or acids, which pose environmental risks and filtration issues (Kupka et al., 2020; Dong et al., 2018; Deng et al., 2019).

Recently, there has been much research on the depression effects of polysaccharides (Liu et al., 2019; Zhou et al., 2021; Zheng et al., 2024; Yang and He, 2025). Some researchers have found that calcium lignosulfonate has a depressing effect on calcite, and the use of calcium lignosulfonate can achieve the separation of fluorite from calcite (Guo et al., 2024). In the separation process of scheelite and calcite, polysaccharides selectively depressed calcite without affecting scheelite flotation. Quebracho has a depressive effect on calcite by adsorbing onto its surface through the complexation of -OH groups with Ca^{2+} ions (Rutledge and Anderson, 2015). Pectin (Jiao et al., 2019) and xanthan gum (Ming et al., 2020; Wang et al., 2020) adsorb onto the calcite surface primarily due to chelation between carboxyl groups and surface calcium species. The adsorption mechanisms of calcium lignosulfonate (Liu et al., 2020; Shun et al., 2019), sodium alginate (Chen et al., 2017), and carboxymethyl chitosan (Feng et al., 2019; Yu et al., 2024) on calcite surfaces primarily involve chemical interactions induced by calcium ions exposed on the calcite surface. Psyllium seed gum effectively inhibits calcite by interacting with surface calcium ions, which prevents sodium oleate (NaOl) adsorption (Zhou et al., 2020). Current literature generally agrees that calcium ions on the calcite surface are crucial for polysaccharide attraction.

Gum arabic (GA) molecules (Fig. 1) possess a structure termed "Wattle blossom"; each core polypeptide backbone is linked to polysaccharide groups. GA, derived from the dried sap of Acacia trees, comprises pyran galactose, pyran and furan arabinose, pyran rhamnose, pyran glucuronic acid, and 4-O-Methyl pyran glucuronic acid (Liu et al., 2020; Zhong et al., 2022; Wang et al., 2023). It finds applications in the food industry as a thickener, stabilizer, and textured additive. In the field of flotation, Wang et al. used gum arabic as a selective depressant to separate specularite from chlorite. Liu et al. achieved the separation of chalcopyrite from talc using gum arabic, and Zhong et al. discovered that gum arabic can selectively depress calcite in the flotation of apatite and calcite. This study aims to evaluate its application in scheelite froth flotation, as no prior research has been conducted in this area.

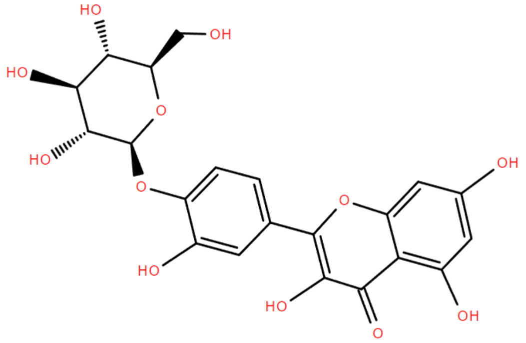

Fig. 1. Structure of gum arabic molecules

2. Experimental materials and methods

2.1. Samples and reagents

The scheelite and calcite samples are crushed to small particle size and then manually selected for high purity samples. The scheelite samples are further ground to the feed size of the shaking table (2mm) and then purified. X-ray diffraction (XRD) patterns show that the purity of the scheelite samples is high, with only trace amounts of silicate detected in the calcite (Fig. 2). The XRD pattern indicates that the primary exposed surfaces of scheelite and calcite during crushing or grinding are {112}, {101}, and {104}, and literature has indicated that the density of calcium ions on the surface of calcite is higher than that of scheelite for these crystallographic planes, with detailed data presented in Table 1(Gao et al., 2018).

The test results show that the content of WO_3 in scheelite samples is 79.80%, with a purity of 99.10%. Calcite samples contain 55.47% calcium oxide with a purity of 99.0% (Table 2). Scheelite/calcite coarse particles were further ground with a porcelain ball mill. Mineral particles smaller than 38μm were acquired through wet screening. Flotation, adsorption, Zeta potential, and X-ray photoelectron spectroscopy (XPS) tests were performed on samples with particle sizes below 38μm. Sodium oleate (≥97%) and pharmaceutical-grade GA (MW 300,000) were obtained from Aladdin Chemical Technology Co., Ltd. The experiment utilized analytical grade HCl and NaOH, with all procedures conducted in deionized water.

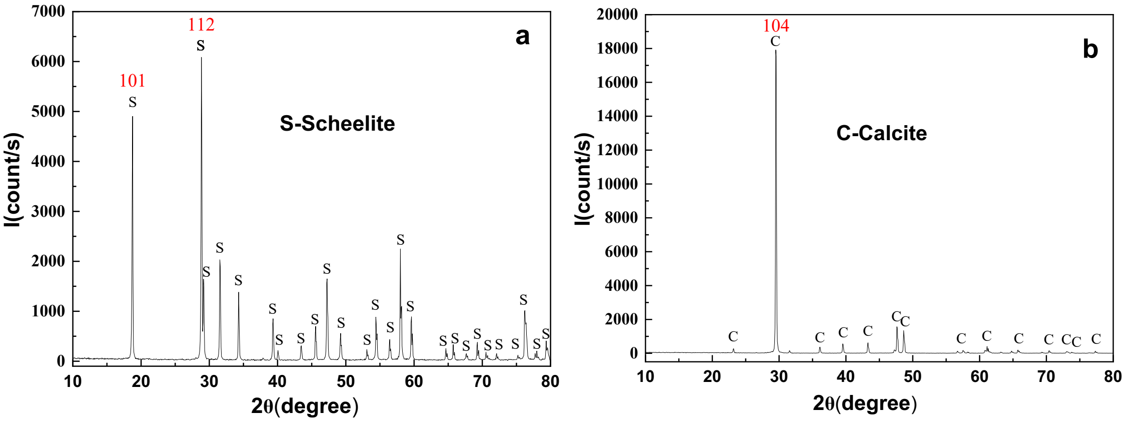

Fig. 2. XRD spectra of the samples: (a) scheelite and (b) calcite

Table 1. Ca densities on exposed planes of calcite and scheelite

Mineral surface	Surface unit cell area, nm^2	Number of Ca atoms in each unit cell area	Ca density, μmol/m^2
Calcite {104}	0.404	2	8.22
Scheelite {112}	0.504	2	6.58
Scheelite {101}	0.328	1	5.06

Table 2. Chemical compositions of samples

Sample	WO_3 (%)	Fe (%)	SiO_2 (%)	Al_2O_3 (%)	CaO (%)	Purity
Scheelite	79.80	/	/	/	19.72	99.10%
Calcite	/	0.21	0.52	0.22	55.47	99.00%

2.2. Preparation of microbubbles

The device for generating microbubbles is shown in Fig. 3, which consists of a closed system connected by a peristaltic pump (Leadfluid WG600S) and a rubber tube (diameter of 7mm). Deionized water is added to the bubble generator after being adjusted with reagents to achieve circulatory cavitation by means of a peristaltic pump. When the solution passes through the constriction of the Venturi tube, due to the significant reduction in the liquid flow cross-sectional area, the internal pressure of the liquid is lower than the gas dissolved saturation vapor pressure, and gas nuclei precipitate in the form of microbubbles, achieving cavitation (Wu et al., 2022; Zhang et al., 2021). During the cavitation process, the peristaltic pump operates at a speed of 300 rpm, and the cavitation time is 4min. The bubble size measurement device uses the Brookhaven 90 Plus nano particle size and Zeta potential analyzer. 30mL of cavitated solution is used for measurement, and all cavitated bubbles are used immediately to prevent coalescence and rupture over time. Each sample group is tested thrice, and the mean value is used as the final result. Fig. 4 illustrates the average particle size measured, aligning with the typical microbubble size of generally under several hundred micrometers.

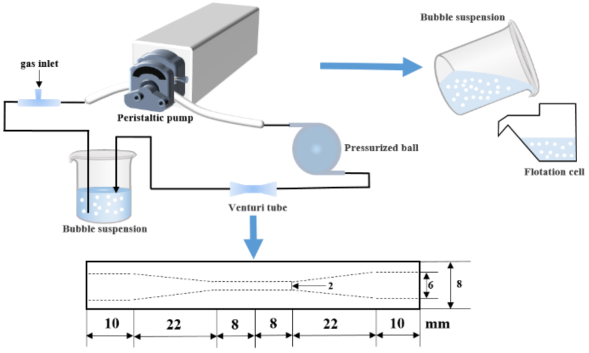

Fig. 3. Microbubbles generator

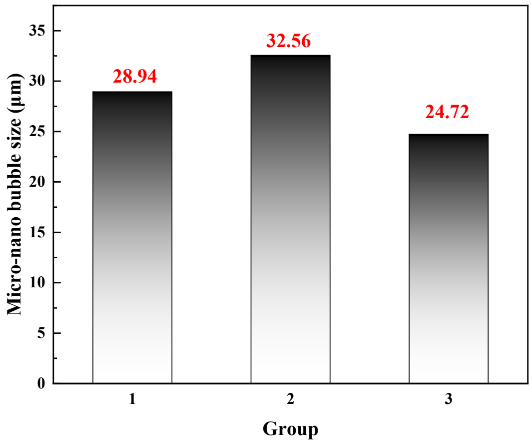

Fig. 4. Average size of hollowed air bubbles

2.3. Flotation test

Micro-flotation tests for individual minerals and binary-mixture minerals were carried out to verify the selective depression ability of GA for calcite. Flotation tests were performed with an XFG flotation machine equipped with a 40mL cell, maintaining a stirring speed of 1908rpm. Each mineral flotation test adding 2g of either scheelite or calcite sample and 30mL of deionized water or bubble suspension to the flotation cell. The pH was set to the target level using a 0.01mol/L aqueous solution of HCl or NaOH. GA and NaOl were used as depressant and collector, respectively. The slurry was initially adjusted for 3min, after which an appropriate amount of GA solution was added with continuous stirring for another 3min, followed by a pH adjustment within 2min. Finally, NaOl was added to the slurry and stirred for 3min. The foam was collected for 4min. The concentrate was dried and weighed to calculate the recovery of scheelite or calcite.

The above-mentioned flotation process was carried out for the binary mixed minerals. Calcite and scheelite were mixed in a 1:1 ratio as feed samples. The concentrates and tailings were ultimately collected and analyzed.

2.4. Adsorption test

Samples for the adsorption tests were added to 100mL of ethyl alcohol, followed by stirring, and then passed through a 5μm filter membrane. After filtration, the samples were vacuum-dried at 120℃. This process was repeated thrice to reduce contamination by organic carbon. The specific surface area of the samples was measured using an automated physisorption apparatus. The samples for specific surface area measurements were ground to a size of 38μm, and the measured specific surface areas of scheelite and calcite were 0.6492 and 1.5389m^2/g, respectively.

The depressant adsorption capacity was measured with a total organic carbon (TOC) analyzer (Elementar Vario TOC, Germany, Elementar Co.). Mix 1g of scheelite/calcite was combined with 100mL of deionized water and stirred thoroughly. The slurry pH was set to the desired level before adding the necessary amount of depressant solution. The slurry was then stirred and allowed to settle, and the supernatants were collected and centrifuged at a rotation speed of 6400rpm in a high-speed centrifuge to remove the fine particles. Following centrifugation, the liquid was filtered through a 0.45μm membrane to prepare the test sample. The adsorbed quantity on the scheelite/calcite surface was determined by deducting the GA amount in the supernatant from the total GA amount. The calculation formula for the adsorption density is given by Eq. (2).

$$\Gamma = \frac{v(c_0 - c)}{mA} \tag{2}$$

where Γ is the adsorption density of GA (mg/m^2), c_0 and c represent the total and supernatant concentrations (mg/L), v is the slurry volume (L), m denotes the mineral sample weight (g), and A is the specific surface area of the mineral powder (m^2/g).

2.5. Measurement of zeta potential

Zeta potential was measured using a ZetaPALS analyzer (Brookhaven). Mineral suspensions were created by combining 1g of mineral samples with 50ml of deionized water, followed by the addition of 1ml of 5×10^{-2}mol/L KNO_3 as an electrolyte. The suspension pH was adjusted to 9.0 by adding NaOH or HCl aqueous solution. The GA/NaOL solution was added to the slurry until the desired concentration was reached, after which it was transferred to the measuring cell. The final Zeta potential value was calculated as the average of three consecutive measurements (microbubbles potential can be measured after adding the reagents).

2.6. Contact angle measurement

Select two ore blocks with good crystallinity, and use a cutting machine to cut each block into two planes. By using a fine grinding. Sand paper polish and polish until the surface is smooth. Place the ore block into a beaker containing a suitable amount of deionized water, and use ultrasound. Washing the samples with water and air drying naturally. The contact angles of scheelite and calcite were assessed using a contact angle measuring instrument. Ore samples were soaked for 2 hours under optimal flotation conditions, determined by single mineral analysis, using specific reagent concentrations. Subsequently, the samples were washed multiple times with deionized water, allowed to dry naturally, and then their contact angles were measured.

2.7. XPS test

XPS tests were conducted using a Thermo Fisher K-Alpha X-ray photoelectron spectrometer (USA) with a monochromatic Al Kα X-ray source. Samples were moved to an analytical chamber with a vacuum pressure below 3×10^{-8}Pa for high-resolution scanning using an electron energy analyzer set at a 50eV pass energy and a 0.1eV step size.

Prepare the test sample by combining 1g of scheelite/calcite with 50mL of deionized water, adjusting the pH, and incorporating the specified GA concentration. Mix thoroughly, then filter the slurry using a filter membrane. Dry the remaining solid as the experimental sample. Process the data using XPS Avantage software, set the C1s peak at 284.80eV, and calibrate the spectra.

3. Results and analysis

3.1. Flotation test

The floatability of fine scheelite/calcite was studied at different pH values in both conventional bubble system and microbubbles system, and the recovery graph was plotted, as shown in Fig. 5(A). With NaOL as a collector at a concentration of 1.2×10^{-4}mol/L, scheelite recovery exceeded 70% in the pH range of 7 to 11, peaking at 74.5% at pH 9, while calcite recovery was consistently above 80%, even without microbubbles. In the presence of microbubbles in the mineral pulp environment, the recovery of both minerals was improved, with the flotation enhancement effect on scheelite being particularly significant. Specifically, at pH 9, the recovery of scheelite increased by 14.3% to reach 88.8%, while the recovery of calcite was 90.8%, only increasing by 4.5%. Therefore, the presence of microbubbles can effectively recover fine scheelite, and subsequent flotation experiments were all conducted in the microbubble system.

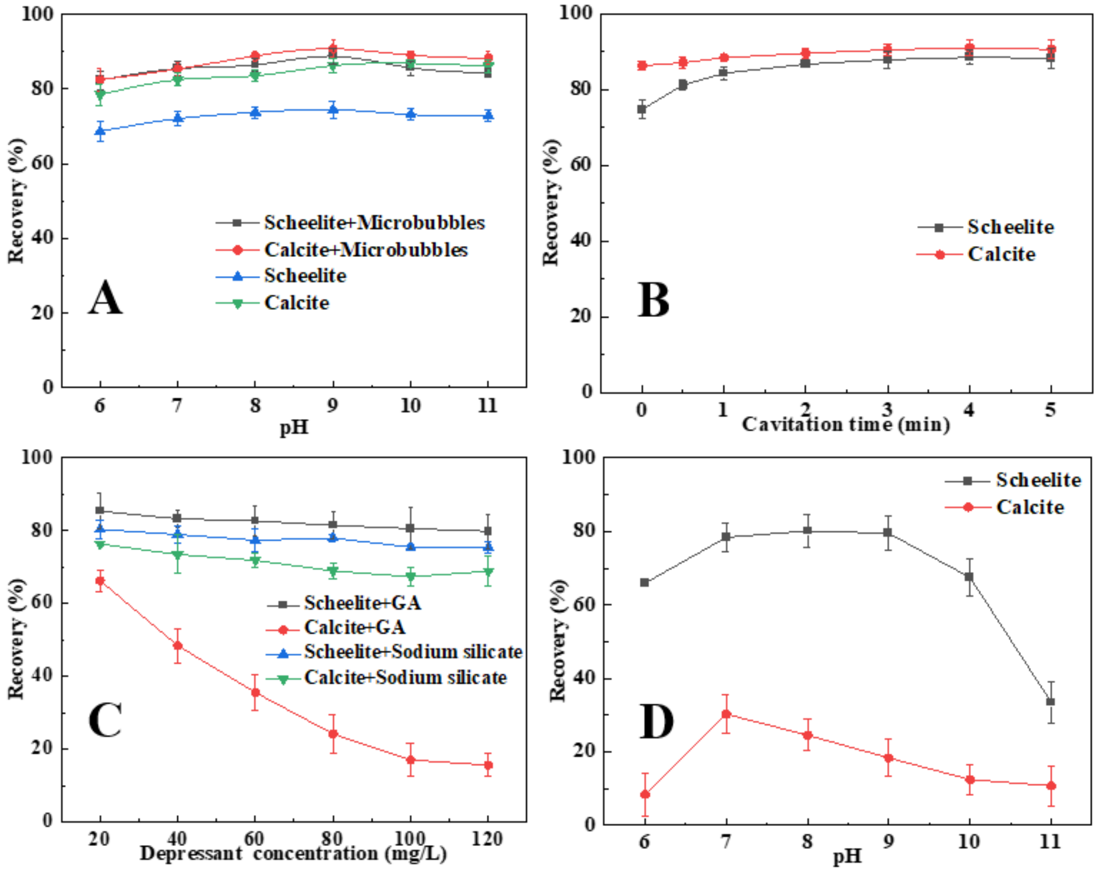

Fig. 5. (A) Effect of microbubbles on scheelite and calcite flotation recovery across varying pH levels, (B) Effect of cavitation time on scheelite and calcite flotation recovery, (C) Microbubble System: Depressant concentration effect on scheelite and calcite flotation recovery, (D) Microbubble System: pH levels effect on scheelite and calcite flotation recovery

Fig. 5(B) shows the effect of cavitation time on the recovery rates of fine-grained scheelite and calcite. In the early stage of the experiment, the average size of microbubbles was measured with cavitation times ranging from 0 to 5min. Millimeter-sized bubbles that were not cavitated transformed into micron-sized bubbles through cavitation, and as the cavitation time increased, the average size of the microbubbles continuously decreased. At 4min, a balance was reached, with an average size distribution ranging from 133.9 to 28.6μm. It can be observed that under the same flotation conditions, as the average size of the microbubbles decreased, the recovery rates of both scheelite and calcite showed an increasing trend, indicating that smaller microbubbles have an advantage in the flotation of fine-grained minerals. This is because smaller bubbles have higher stability, are less prone to rupture, and rise more slowly, resulting in higher collision efficiency, which effectively captures fine-grained minerals.

Fig. 5(C) shows the effect of depressant dosage on the recovery of fine-grained scheelite and calcite under Microbubble System. A comparative study was performed at a constant pH of 9 and a NaOL concentration of 1.2×10^{-4}mol/L. As GA concentration increased, calcite recovery significantly declined, whereas scheelite recovery remained largely unaffected. At a GA dosage of 100mg/L, calcite recovery dropped to 17%, a reduction of approximately 70%, while scheelite recovery was 80.5%. Further increasing the dosage did not significantly enhance the depressive effect. Both scheelite and calcite were depressed by sodium silicate, and when the dosage was less than 100mg/L, it was difficult to separate scheelite from calcite. This indicates that GA offers notable benefits compared to traditional scheelite flotation depressants like sodium silicate.

Fig. 5(D) shows the effect of GA(c(GA) =100mg/L) on the recovery of fine-grained scheelite and calcite at different pH values under Microbubble System. GA exhibits strong inhibition on calcite at pH 6, which may be caused by the addition of HCl solution. Calcite recovery significantly declines within a pH range of 7 to 10, dropping to approximately 10% at pH levels of 10 and 11. Scheelite shows slight inhibition at pH 6, with a recovery exceeding 80% at pH 7 to 9. Notably, the flotation recovery of scheelite drastically drops to 33.5% at pH 10 to 11, indicating an inhibiting effect of scheelite in highly alkaline slurry.

3.2. Mixed mineral flotation test

Based on earlier individual-mineral micro-flotation tests, calcite and scheelite can be separated by adjusting the pH to around 9. GA was employed as a depressant to separate a scheelite-calcite mixture (1:1 weight ratio) to confirm its selective depression efficacy. Table 3 presents the test results. Following the addition of 60 mg/L of GA, a concentrate with 60.47% grade WO_3 and 74.29% scheelite recovery was achieved. The separation of artificially mixed minerals could not be achieved without adding GA as the WO_3 grade and recovery were only 41.43% and 57.42%, respectively.

Table 3. Evaluation of separation effect of GA on mixed minerals (pH:9, NaOL: 1.2×10^{-4}mol/L)

Reagent	Original grade (%)	Yield (%)	WO_3 grade (%)	WO_3 recovery (%)
Gum arabic (60 mg/L)	39.90	49.02	60.47	74.29
None	39.90	55.30	41.43	57.42

3.3. Adsorption behavior of gum arabic on the surfaces of calcite and scheelite.

The amount of GA in the supernatant was determined using the TOC analyzer according to the standard curve shown in Fig. 6(A). The equation for the standard curve is: $Y=0.416+0.249X$, with a fitting variance $R^2=0.99149$. The ability of scheelite and calcite to adsorb GA at different GA doses was obtained through the calculation of formula (2), as shown in Fig. 6(B). As the GA dosage increased, its adsorption capacity on the calcite surface grew more significantly than on scheelite. The adsorption of GA on scheelite was less than on calcite.

3.4. Measurement of zeta potential

The effects of GA and NaOL on the microbubble Zeta potential were recorded and plotted (Fig. 7). Addition of GA solution resulted in a negative shift in microbubble Zeta potential, as GA is an anionic polysaccharide with strong negative charge at pH 6-11. Consequently, the adsorption of GA on microbubbles shifted their surface potential negatively. When the GA concentration was 100mg/L, the Zeta potential of microbubbles decreased by nearly 7mV. Due to NaOL being an anionic collector, the addition of NaOL further decreased the microbubble potential. Under low NaOL conditions, the decrease in microbubble potential slowed down with increasing GA dosage, and after increasing the NaOL dosage, the potential started to approach each other, possibly because GA to some extent hindered NaOL adsorption on microbubbles.

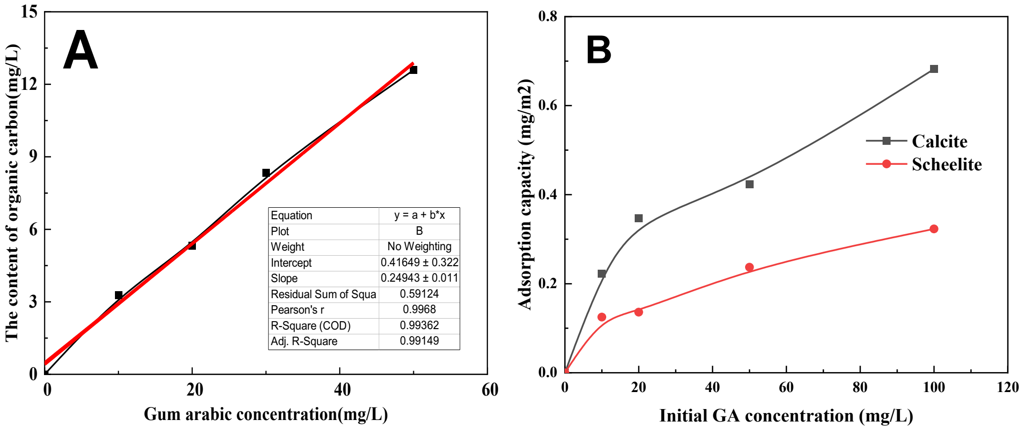

Equation	y = a + b*x
Plot	B
Weight	No Weighting
Intercept	0.41649 ± 0.322
Slope	0.24943 ± 0.011
Residual Sum of Squa	0.59124
Pearson's r	0.9968
R-Square (COD)	0.99362
Adj. R-Square	0.99149

Fig. 6. (A)Standard total organic carbon curve of gum arabic (GA), (B) Capacity of GA on scheelite and calcite surfaces at varying dosages

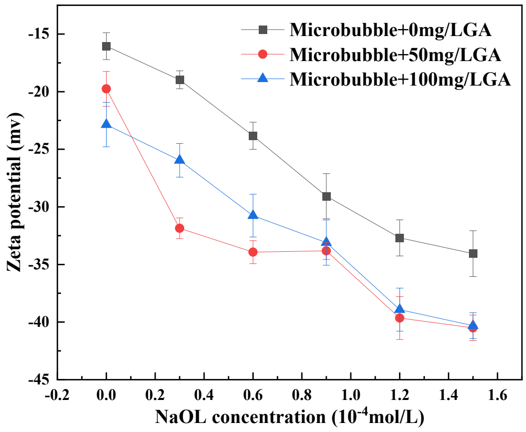

Fig. 7. The variation of Zeta potential of microbubble with the dosage of NaOL (pH: 9)

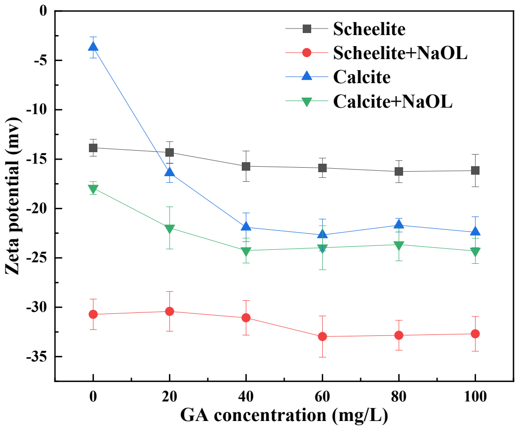

Fig. 8. The Zeta potential of scheelite and calcite varies with the concentration of GA, (pH:9, NaOL: 1.2×10^{-4}mol/L)

Fig. 8 shows the effect of GA concentration on the surface potential of scheelite and calcite as measured by Zeta potential. Increasing GA dosage resulted in a maximum negative potential displacement of 2.41mV on scheelite, significantly less than the 18.99mV observed on calcite. This suggests strong chemical adsorption of GA on calcite, causing a notable negative shift in surface potential, whereas scheelite experienced only weak physical adsorption with minimal potential change. After the action of GA on both minerals, the addition of NaOL caused a sharp negative shift of approximately 15mV on the surface potential of scheelite (Li et al., 2023), whereas calcite only exhibited significant potential changes at low GA dosages, with a displacement of only about 2mV at dosages of 40 to 100mg/L. These results suggest that GA, as an anion, adsorbs on both minerals with a stronger interaction with calcite compared to NaOL. Competitive adsorption hinders NaOL from effectively adsorbing onto calcite surfaces, whereas GA's weaker interaction with scheelite allows its replacement by NaOL. The inclusion of these anions in micro-flotation modifies the electrochemical characteristics of microbubbles, with NaOL predominantly adsorbing on their surface. The introduction of microbubbles selectively adsorbs onto scheelite surfaces, improving flotation separation.

3.5. Contact angle analysis

Fig. 9 illustrates the contact angles of scheelite and calcite before and after their reactions with GA and NaOL. The findings demonstrate that scheelite and calcite are inherently hydrophilic, with contact angles of 34.6° and 47.4°, respectively, rendering them non-recoverable without collectors. The addition of GA significantly reduced the contact angle of calcite to 20.9°, demonstrating enhanced hydrophilicity, whereas the contact angle of scheelite changed by only 2.8°, indicating a minimal effect. The introduction of NaOL raised the contact angle of scheelite to 72.8°, markedly enhancing its floatability. This indicates that GA molecules can adhere to the surface of scheelite through physical adsorption, while not significantly adsorbing onto its active sites to form hydrophilic groups, the wettability of the surface of scheelite only undergoes slight changes, thus avoiding strong hydrophilicity affecting its interaction with sodium oleate. The contact angle of calcite increased with NaOL but stayed slightly below its natural level, indicating that GA enhances calcite's hydrophilicity and partially inhibits NaOL adsorption on its surface.

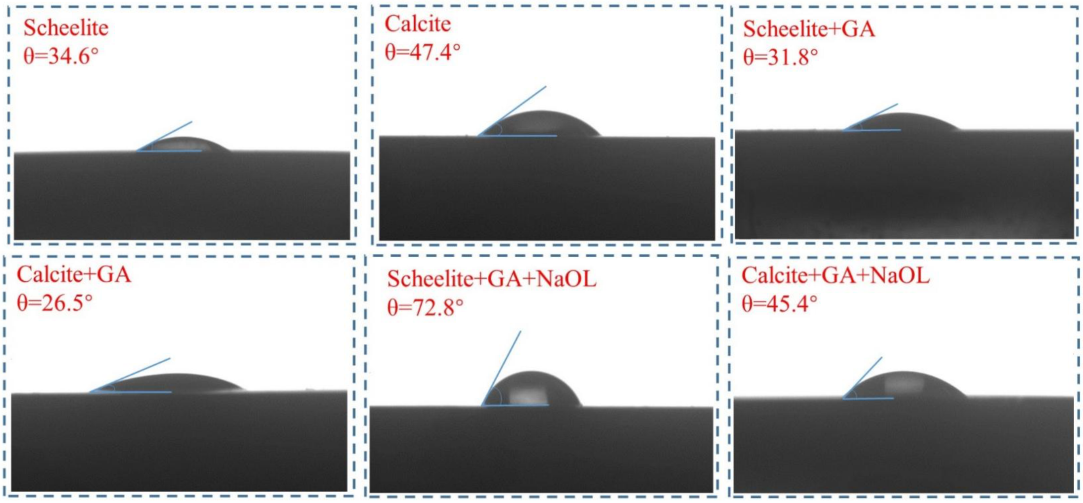

Fig. 9. The contact angle of scheelite and calcite before and after reaction with flotation reagents (pH: 9, GA: 100 mg/L, NaOL: 1.2×10^{-4}mol/L)

3.6. XPS analysis

The figure presents high-resolution C 1s XPS spectra for the two minerals, both with and without GA treatment. The distinct peaks at 284.80eV and 288.48eV in the C 1s spectrum of scheelite, as shown in Fig. 10(A), are attributed to air contamination during preparation, leading to the presence of hydrocarbons and carbon dioxide on the surface. After GA treatment, the peaks shift, which is also attributed to the contamination (Li et al., 2023). Calcite displays two distinct peaks at binding energies of 289.38eV and 284.80eV (Fig. 10(B)). These two peaks can be ascribed to calcium carbonate ($CaCO_3$) and carbon contamination (Zhong et al.2022). The treatment of calcite with GA resulted in a peak at 286.09eV, corresponding to −COO−, a structural feature of GA, confirming its adsorption on the calcite surface.

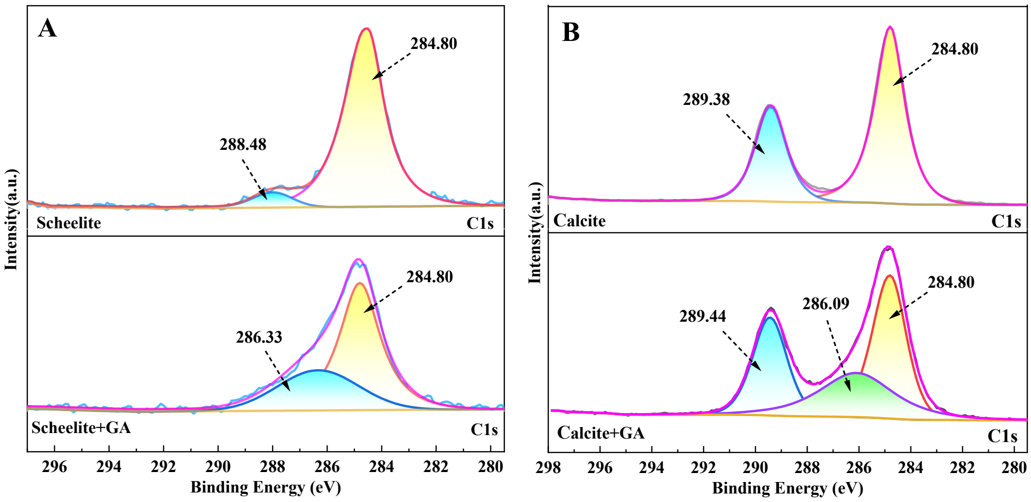

Fig. 10. XPS C 1s spectra for scheelite and calcite, both pre- and post-GA treatment

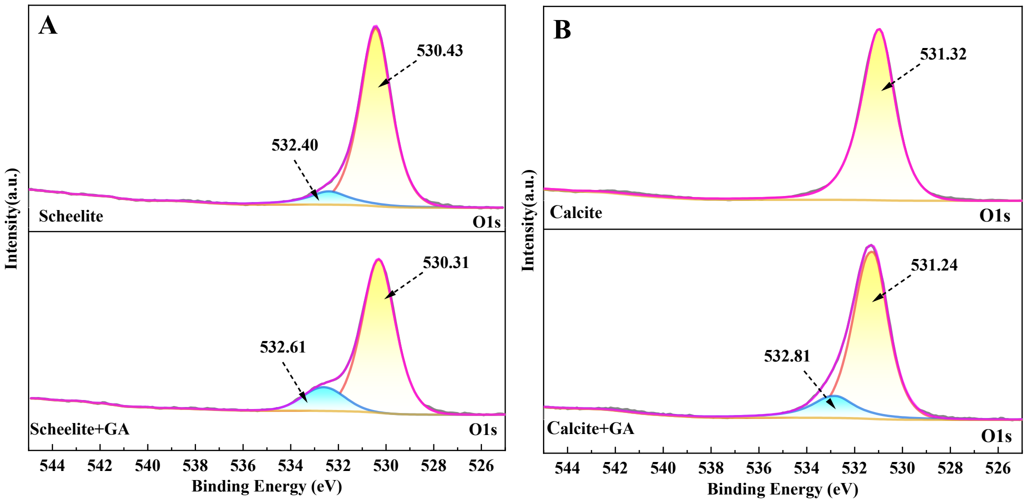

Fig. 11. XPS O 1s spectra for scheelite and calcite, both pre- and post-GA treatment

The Fig. 11 presents the high-resolution XPS spectra for the O 1s of two minerals. As can be seen in Fig. 11(A), the two characteristic peaks of scheelite are 530.43eV and 532.40eV respectively (Zheng et al. 2025), and the two peaks shift slightly after adding GA, and the intensity changes at 532.61ev, indicating that GA produces weak physical adsorption of scheelite. Calcite exhibits a peak at 531.32eV (Fig. 11(B)), and following interaction with the further increasing the dosage did not significantly enhance the depressive effect. GA, a new peak emerges at 532.81eV, attributed to the -OH group in the GA molecule (Zhou et al., 2020). This demonstrates that GA is chemically adsorbed onto calcite, showing that the -OH groups in GA effectively chelate with surface Ca^{2+} ions. This is consistent with the strong inhibition of calcite in the micro-flotation experiment.

Fig. 12 presents the high-resolution XPS spectra of Ca 2p prior to and following the introduction of two minerals. The characteristic peaks of scheelite are 346.88eV and 350.46eV (Zhong et al. 2021), and after the addition of GA, the two peaks exhibit slight shifts (Fig. 12(A)). The binding energies of Ca 2p3/2 and Ca 2p1/2 on calcite are 346.86eV and 350.44eV, indicating two characteristic peaks. After GA treatment, the characteristic peaks appear at binding energies of 347.00eV and 350.40eV for Ca 2p3/2 and Ca 2p1/2, showing changes of 0.14eV and 0.04eV. A new peak is observed at 346.06eV (Fig. 12(B)), which could be Ca-COOR (Dong et al. 2019), indicating chelation between the carboxyl group (-COO-) of GA molecules and the calcium ions on calcite surfaces.

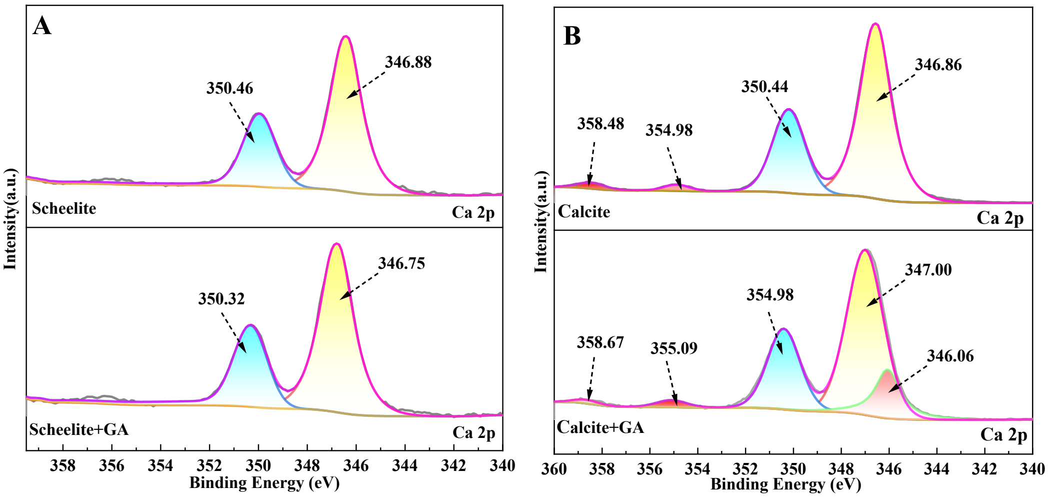

Fig. 12. XPS Ca 2p spectra for scheelite and calcite, both pre- and post-GA treatment

3.7. EDLVO calculation

The EDLVO calculations depicting the interaction forces between bubbles and scheelite/calcite, as illustrated in Fig. 13, incorporate potential values and mineral contact angle parameters derived from Sections 3.4 and 3.5. These parameters were measured under conditions where the reagent concentration was C(NaOL)=1.2×10×$^{-4}$mol/L and the dosage of GA was 100mg/L. We found that as the bubble size increases, the repulsion between the bubbles and scheelite/calcite becomes more pronounced, indicating that bubbles in the tens of micrometers range can adhere well to scheelite in the flotation system. When using GA as a depressant, the potential of calcite shows a slight increase, while the contact angle decreases significantly. This leads to a substantial enhancement of the repulsion between the bubbles and calcite, further confirming that bubbles can adhere to the surface of scheelite but find it difficult to adhere to the surface of calcite. This suggests that the addition of GA enables selective adhesion of bubbles to scheelite.

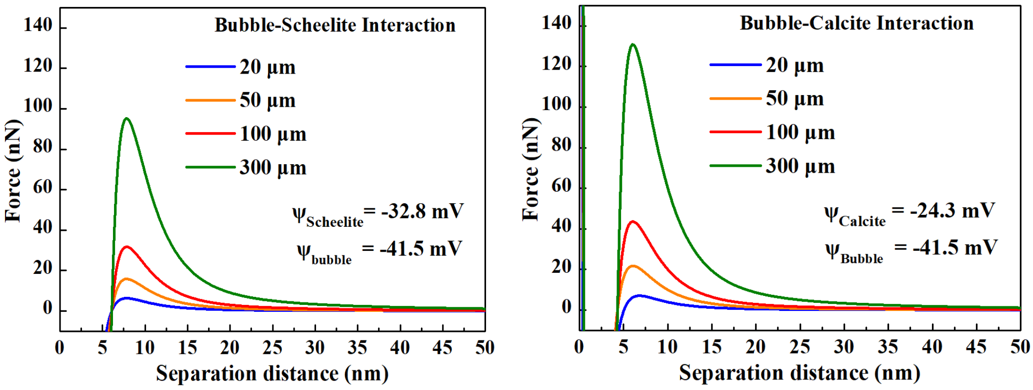

Fig. 13. EDLVO calculation of the interaction force between scheelite/calcite and bubbles in various size

4. Discussion

In this study, the combined use of microbubbles and gum arabic not only enhanced the selective depression ability of gum arabic on calcite but also improved the recovery rate of scheelite. This is because the addition of gum arabic significantly expanded the hydrophobicity difference between scheelite and calcite, allowing most microbubbles to selectively adhere to the surface of scheelite, thereby increasing its recovery rate. Compared to traditional flotation, the use of microbubbles can effectively increase the floatability of fine scheelite particles, as microbubbles have a smaller volume and relatively higher Laplace pressure, making it easier for them to adhere to the surface of fine scheelite particles, allowing them to rise to the surface of the flotation tank and form a froth layer, thus improving the recovery rate. The generation of microbubbles also enhances the contact rate between bubbles and scheelite particles, allowing fine scheelite to be more easily captured by the bubbles, which contributes to increased flotation efficiency. Additionally, the presence of microbubbles can improve the distribution and effectiveness of flotation reagents, enhancing the hydrophobicity of scheelite surfaces and facilitating the flotation process.

In the flotation separation process, the adsorption capacities of scheelite and calcite on GA vary primarily due to the differing calcium densities on their exposed surfaces, leading to distinct surface calcium concentrations (Table 1). GA, a polysaccharide, possesses numerous carboxylic (-COO-) and hydroxyl (-OH) groups capable of chelating with Ca^{2+} on calcite surfaces, affecting its surface properties, enhancing its hydrophilicity and thereby reducing its floatability. The interaction of these anions with Ca^{2+} also serves as a charge neutralization, reducing the surface energy of calcite and thereby diminishing the ability of bubbles to adhere to the mineral, inhibiting its flotation. At the same time, a layer of adsorbed film may form on the surface of calcite, obstructing the contact between the collector and the mineral surface, thus decreasing flotation efficiency. XPS test results also confirm that the main adsorption mechanism of calcite with GA is chelation, while GA mainly undergoes physical adsorption on scheelite. Through EDLVO calculations, it is concluded that after GA adsorption, the difference in hydrophobicity between scheelite and calcite significantly increases. Bubbles at the micrometer level can adhere well to scheelite, but the repulsive force between them and calcite is significantly strengthened. This indicates that bubbles can adhere to the surface of scheelite but find it difficult to adhere to the surface of calcite, proving that the addition of GA facilitates selective adhesion of bubbles to scheelite, thereby enhancing the separation efficiency of flotation. Fig. 14 illustrates the potential adsorption mechanism of GA/microbubbles on calcite and scheelite.

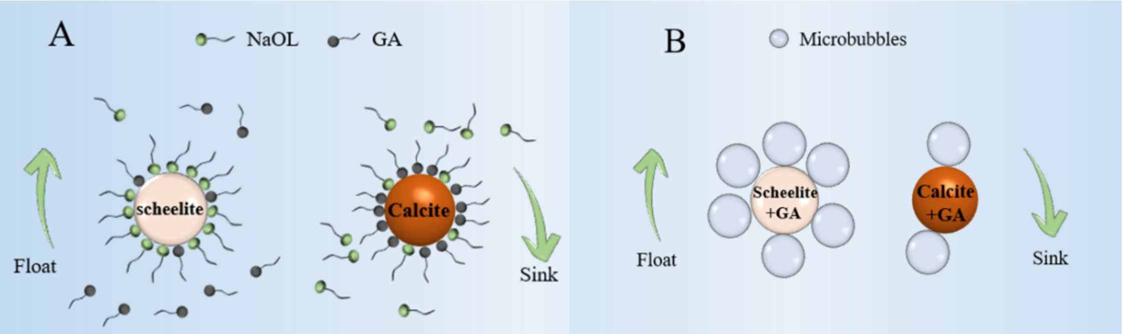

Fig. 14. Illustration of the (A)GA; (B)Microbubbles adsorption behavior of calcite and scheelite surfaces

5. Conclusions

(1) Microbubbles can effectively improve the flotation of fine-grained scheelite, with limited effect on fine-grained calcite. GA effectively inhibits calcite between pH 7 and 9 without affecting scheelite's floatability. Mixed mineral flotation experiments have shown that under pH=9.0 conditions, GA as a depressant can achieve the flotation separation of fine-grained scheelite and calcite. A concentrate with a WO_3 grade of 60.47% and a recovery rate of 74.29% is achievable from a mixed mineral with a WO_3 grade of 39.9%.

(2) The contact angle measurement results show that GA can hydrophilize calcite and to some extent inhibit the adsorption of collectors on the calcite surface, with no significant effect on scheelite.

(3) Zeta potential measurements indicate that GA preferentially competes with NaOL for adsorption on calcite surfaces, while both GA and NaOL modify microbubble electrification, leading to selective adsorption on scheelite surfaces and improving flotation separation efficiency.

(4) XPS and adsorption experiments analysis show that GA can be adsorbed on both calcite and scheelite surfaces, with the adsorption capacity on calcite surface greater than on scheelite surface, mainly due to the higher atomic density of Ca on the calcite surface. GA exhibits weak physical adsorption on scheelite and strong chemical adsorption on calcite.

(5) GA, as an environmentally friendly alternative to traditional depressants, has lower toxicity and is biodegradable. Compared to conventional chemical inhibitors, the use of GA can effectively reduce pollution to water bodies and soil, alleviating the pressure on ecosystems. Additionally, the application of GA can enhance selectivity in the flotation process, improving the efficiency of mineral separation. By optimizing flotation processes, GA can achieve greater economic and environmental benefits.

Acknowledgments

This work was supported by the financial support from the Special Project for Cultivating Young Talents in Science&Technology in the Early Stage in Jiangxi province (Grant no. 20244BCE52187); the Jiangxi Provincial Department of Science and Technology Carbon Peak and Carbon Neutrality Science and Technology Innovation Special Project (grant no. 20214BBG74001);

References

BEN SAID, B., RUDOLPH, M., Ebert, D., GOLDMANN, D., PEREIRA, L., 2024. *Nanoparticle depressants in froth flotation – The effect of colloidal silica with different size and surface modifications on the selective separation of semi-soluble salt type minerals*. Colloids Surf., A. 690, 133697.

CHANG, Z., NIU, S., SHEN, Z., ZHOU, L., WANG, H., 2023. *Latest advances and progress in the microbubble flotation of fine minerals: Microbubble preparation, equipment, and applications*. Int. J. Miner., Metall. Mater. 30, 1244–1260.

CHEN, W., FENG, Q., ZHANG, G., YANG, Q., ZHANG, C., 2017. *The effect of sodium alginate on the flotation separation of scheelite from calcite and fluorite*.C113, 1-7.

DENG, J., LIU, C., YANG, S., LI, H., LIU, Y., 2019. *Flotation separation of barite from calcite using acidified water glass as the depressant*. Colloids Surf., A. 579, 123605.

DONG, L., CUI, Y., QIAO, L., LAN, S., ZHENG, Q., SHEN, P., LIU, D., 2025. *A critical review on the flotation of calcium-containing minerals*, Sep. Purif. Technol. 360, 131082.

DONG, L., JIAO, F., QIN, W., ZHU, H., JIA, W., 2018. E*ffect of acidified water glass on the flotation separation of scheelite from calcite using mixed cationic/anionic collectors*. Appl. Surf. Sci. 444, 747-756.

DONG, L., JIAO, F., QIN, W., LIU, W., 2019. *Selective flotation of scheelite from calcite using xanthan gum as depressant*. Miner. Eng. 138, 14-23.

FILIPPOV, L.O., FOUCAUD, Y., FILIPPOVA, I.V., BADAWI, M., 2018. *New reagent formulations for selective flotation of scheelite from a skarn ore with complex calcium minerals gangue*. Miner. Eng. 123, 85-94.

FAWZY, MM., 2018. *Surface characterization and froth flotation of fergusonite from Abu Dob pegmatite using a combination of anionic and nonionic collectors.* Physicochem. Probl. Miner. Process.54(3), 677-687.

FARAMARZPOUR, A., SAMADZADEH YAZDI, M.R., MOHAMMADI, B., CHEHREH CHELGANI, S., 2022. *Calcite in froth flotation - A review*. J. Mater. Res. Technol. 19, 1231-1241.

FENG, B., PENG, J., GUO, W., LUO, G., ZHANG, W., WANG, H., 2019. *The depression behavior and mechanism of carboxymethyl chitosan on calcite flotation*. J. Mater. Res. Technol. 8(1), 1036-1040.

GAO, Y., GAO, Z., SUN, W., YIN, Z., WANG, J., HU, Y., 2018. *Adsorption of a novel reagent scheme on scheelite and calcite causing an effective flotation separation*. J. Colloid Interface Sci. 512, 39-46.

GUO, S., KUANG, J., ZHANG, S., HUANG, Z., 2024. *Effect of calcium lignosulfonate on the interaction forces between fine calcite and fluorite*. Sep. Purif. Technol. 336, 126172.

HUAGN, G., FENG, Q., OU, L., LU, Y., ZHANG, G., 2009. *Recovery of fine-grained scheelite from flotation tailings using microbubble flotation column*. Zhongnan Daxue Xuebao, Ziran Kexueban.40(02), 263-267.

JI, D., LI, J., MA, Z., CHENG, W., 2021. *Application of Combined Column Machine Process in Flotation of a Low-Grade Scheelite Ore in Hunan*. Mineral Resources Protection and Utilization. 41(02), 117-122.

JIAO, F., DONG, L., QIN, W., LIU, W., HU, C., 2019. *Flotation separation of scheelite from calcite using pectin as depressant*. Miner. Eng. 136, 120-128.

KUPKA, N., KADEN, P., JANTSCHKE, A., SCHACH, E., RUDOIPH, M., 2020. *Acidified water glass in the selective flotation of scheelite from calcite, part II: species in solution and related mechanism of the depressant.* Physicochem. Probl. Miner. Process. 56(5), 797-817.

KUPKA, N., RUDOLPH, M., 2018. *Froth flotation of scheelite – A review*. Int. J. Min. Sci. Technol. 28(3), 373-384.

LI, H., AFACAN, A., LIU, Q., XU, Z., 2015. *Study interactions between fine particles and micron size bubbles generated by hydrodynamic cavitation*. Miner. Eng. 84, 106-115.

LI, X., HE, H., ZHANG, Y., WU, Y., GUAN, Z., 2023. *Flotation separation of scheelite from calcite using baicalin as a depressant*. Colloids Surf., A. 675, 132006.

LIU, C., FENG, Q., SHI, Q., ZHANG, W., SONG, S., 2019. *Utilization of N-carboxymethyl chitosan as a selective depressant for talc in flotation of chalcopyrite.* Physicochem. Probl. Miner. Process.55(1), 108-115.

LIU, D., ZHANG, G., HUANG, G., GAO, Y., WANG, M., 2020. *Investigations on the selective flotation of chalcopyrite from talc using gum Arabic as depressant*. Sep. Sci. Technol. 55(18), 3438–3446.

LIU, J., ZHANG, G., LUO, Y., 2020. *Effect of depressants in the selective flotation of smithsonite and calcite using cationic collector*. Physicochem. Probl. Miner. Process. 56(1), 1-10.

LU, Y., DING, R., LI, G., SONG, X., CAO, Y., JIA, K., 2023. *Research Progress with Scheelite Flotation Reagents: A Review.* Minerals., 13(10), 1257.

MIETTINEN, T., RALSTON, J., FORNASIERO, D., 2010. *The limits of fine particle flotation*. Miner. Eng. 23(5), 420-437.

MING, P., XIE, Z., GUAN, Y., WANG, Z., LI, F., XING, Q., 2020. *The effect of polysaccharide depressant xanthan gum on the flotation of arsenopyrite from chlorite*. Miner. Eng. 157, 106551.

PENG, T., TAO, L., WANG, J., DONG, L., JIA, W., WANG, F., HU, J., GAO, Z., 2024. *Selective flotation separation of scheelite from calcite using hexamethylenediamine tetramethylene phosphonic acid as a novel depressant*. J. Mol. Liq. 402, 124569.

QIAO, L., DONG, L., ZHANG, T., SHEN, P., LIU, D., 2024. *Metal ions modified small molecule organic inhibitor to achieve efficient flotation separation of scheelite from calcite.* Adv. Powder Technol. 35, 8, 104557.

RULYOV, N.N., FILIPPOV, L.O., KRAVCHENKO, O.V.,2020. *Combined microflotation of glass beads*, Colloids Surf., A. 598, 124810.

RUTLEDGE, J., ANDERSON, CG., 2015. *Tannins in Mineral Processing and Extractive Metallurgy*. Metals. 5(3), 1520-1542.

SHUN, Q., FENG, Q., SHI, Q.,2019. *Effect of depressants in the selective flotation of smithsonite and calcite using potassium lauryl phosphate as collector.* Physicochem. Probl. Miner. Process. 55(1) ,89-96.

WANG, H., YANG, C., HU, Y., LI, M., 2023. *Selective depression action of gum arabic in flotation separation of specularite and chlorite.* J. Cent. South Univ. 30, 3044–3056.

WANG, J., GAO, Z., GAO, Y., HU, Y., SHUN, W., 2016. *Flotation separation of scheelite from calcite using mixed cationic/anionic collectors*. Miner. Eng. 98, 261-263.

WANG, R., SUN, W., HAN, H., SUN, W., WEI, Z., PENG, J., 2022. *Al-caustic starch coordination compounds: A new depressant for fine calcite.* Colloids Surf., A. 648, 129268.

WANG, Z., WU, H., YANG, J., TANG, Z., LUO, L., SHU, K., XU, Y., XU, L., 2020. *Selective flotation separation of bastnaesite from calcite using xanthan gum as a depressant.* Appl. Surf. Sci. 512, 145714.

WEI, P., REN, L., ZHANG, Y., BAO, S., 2021. *Influence of Microbubble on Fine Wolframite Flotation*. Minerals. 11, 1079.

WU, M., YUAN, S., SONG, H., LI, X., 2022. *Micro-nano bubbles production using a swirling-type venturi bubble generator*, Chem. Eng. Process. 170, 108697.

YANG, B., HE, J., 2025.*New insights into selective depression mechanism of Tamarindus indica kernel gum in flotation separation of fluorapatite and calcite*. Sep. Purif. Technol. 354(3), 128787.

YU, A., DING, Z., YUAN, J., YU, P., CHEN, L., ZHANG, Y., WEN, S., BAI, S., 2024. *Influence of carboxymethyl chitosan on selective flotation separation of smithsonite from calcite with sodium oleate.* Adv. Powder Technol. 35(9), 104604.

ZHANG, Y., WEI, Z., XU, J., WANG, H., ZHU, H., LV, H., 2021. *Numerical simulation and application of micro-nano bubble releaser for irrigation.* Mater. Express. 11(6), 1007-1015.

ZHENG, Q., DONG, L., SHEN, P., LIU, D., 2025. *A novel mixed depressant for the flotation separation of scheelite and cassiterite: Adsorption mechanism and performance.* Sep. Purif. Technol. 356, 129823.

ZHENG, Q., ZHOU, Y., QIAO, L., SHEN, P., MAO, Y., DONG, L., LIU, D., 2024. *Selective adsorption of soluble starch on the cassiterite surface for effective flotation separation of scheelite from cassiterite*. Surf. Interfaces. 48, 104238.

ZHONG, C., FENG, B., ZHANG, L., ZHANG, W., WANG, H., GAO, Z., 2022. *Flotation separation of apatite and calcite using gum arabic as a depressant*, Colloids Surf., A. 632, 127723.

ZHONG, C., WANG, H., FENG, B., ZHANG, L., CHEN, Y., GAO, Z., 2021. *Flotation separation of scheelite and apatite by polysaccharide depressant xanthan gum.* Miner. Eng. 170, 107045.

ZHOU, H., YANG, Z., TANG, X., SHUN, W., GAO, Z., LUO, X., 2021. *Enhancing flotation separation effect of fluorite and calcite with polysaccharide depressant tamarind seed gum.* Colloids Surf., A. 624, 126784.

ZHOU, H., ZHANG, Y., TANG, X., CAO, Y., LUO, X., 2020. *Flotation separation of fluorite from calcite by using psyllium seed gum as depressant*. Miner. Eng. 159, 106514.